Pyroclastic Density Currents

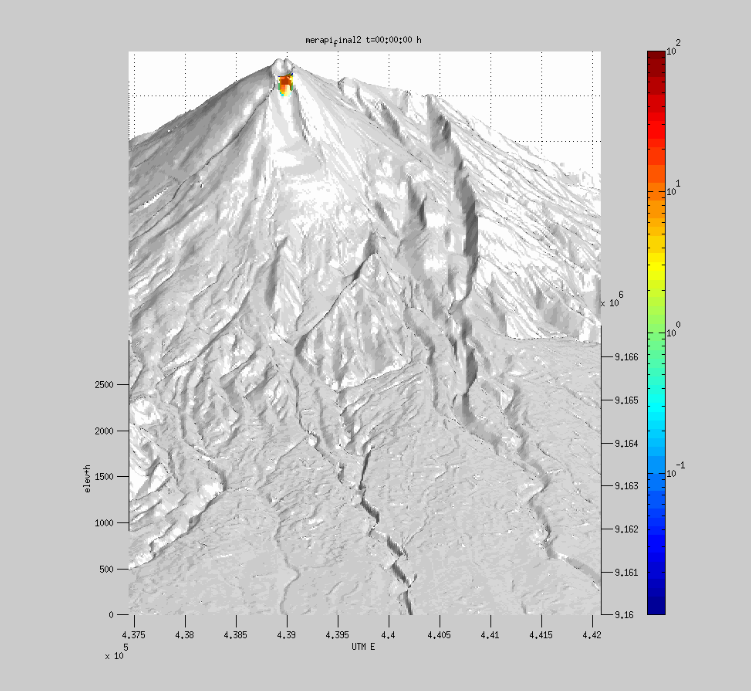

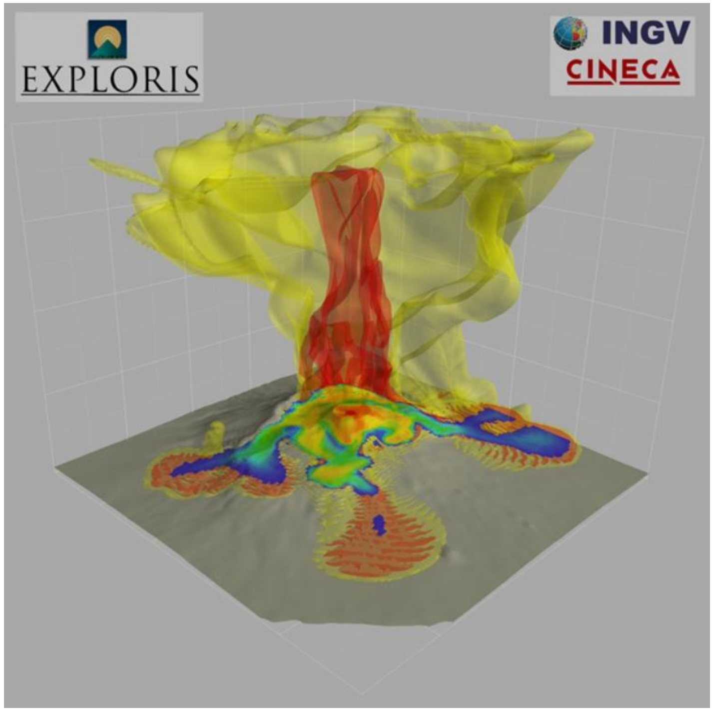

Pyroclastic density currents

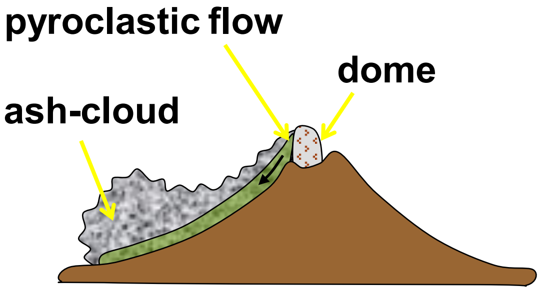

gravitational dome collapse

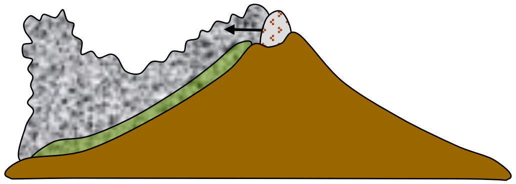

explosive dome or subsurface (crypto-) dome collapse

Generation mechanisms

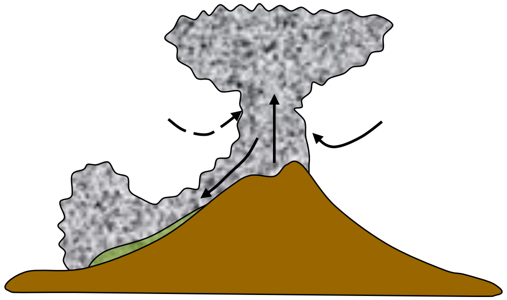

collapse of column

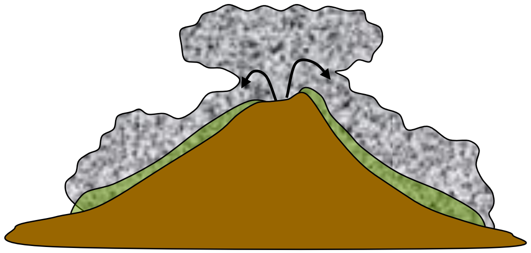

fountaining at vent

Towards a new transport model for PDCs…

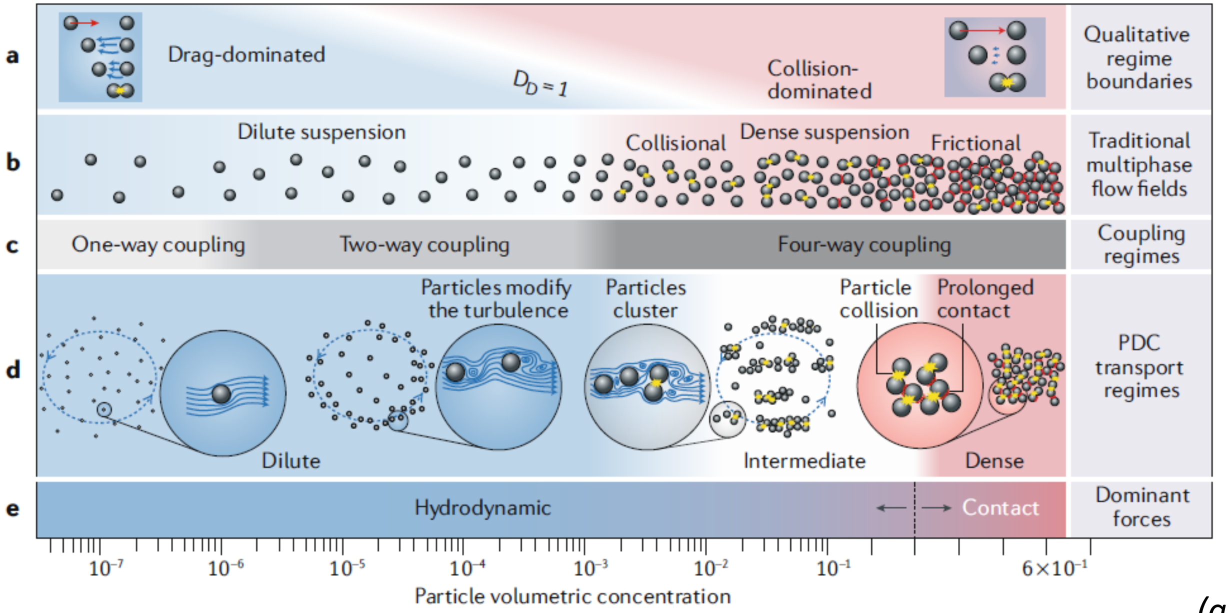

(after Lube et al., 2020)

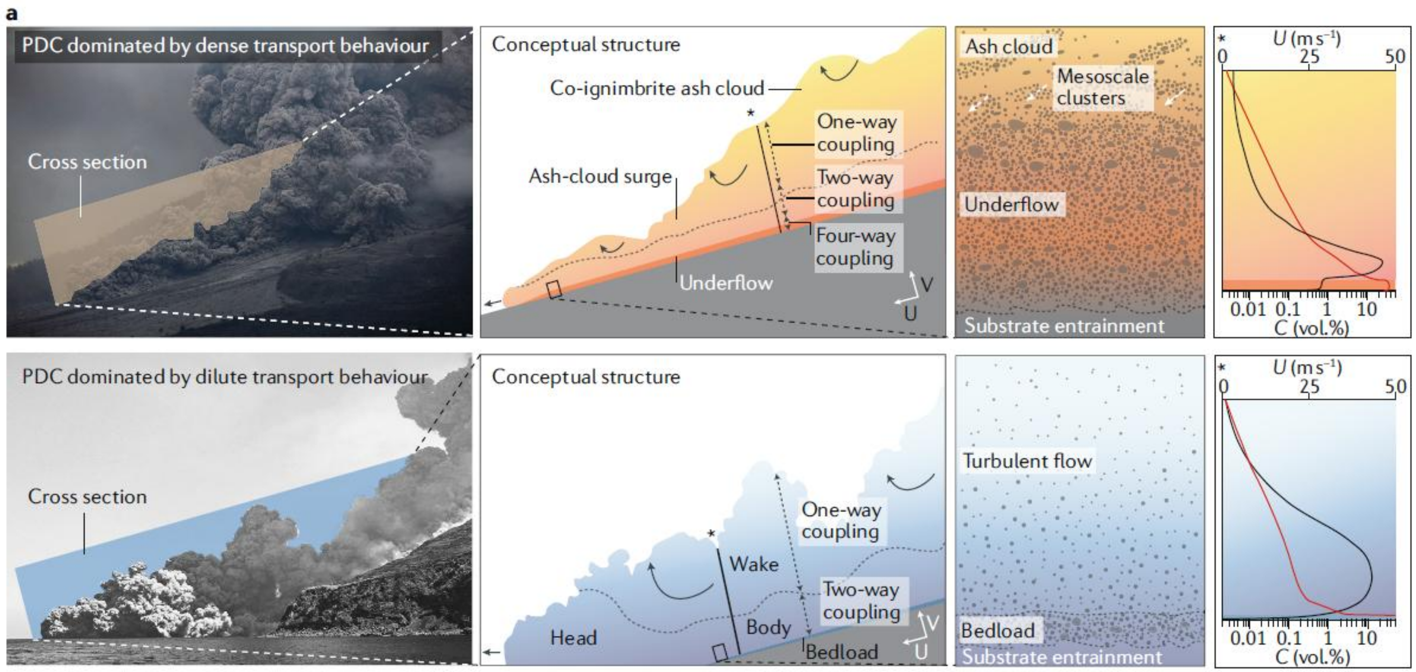

Some PDC models available

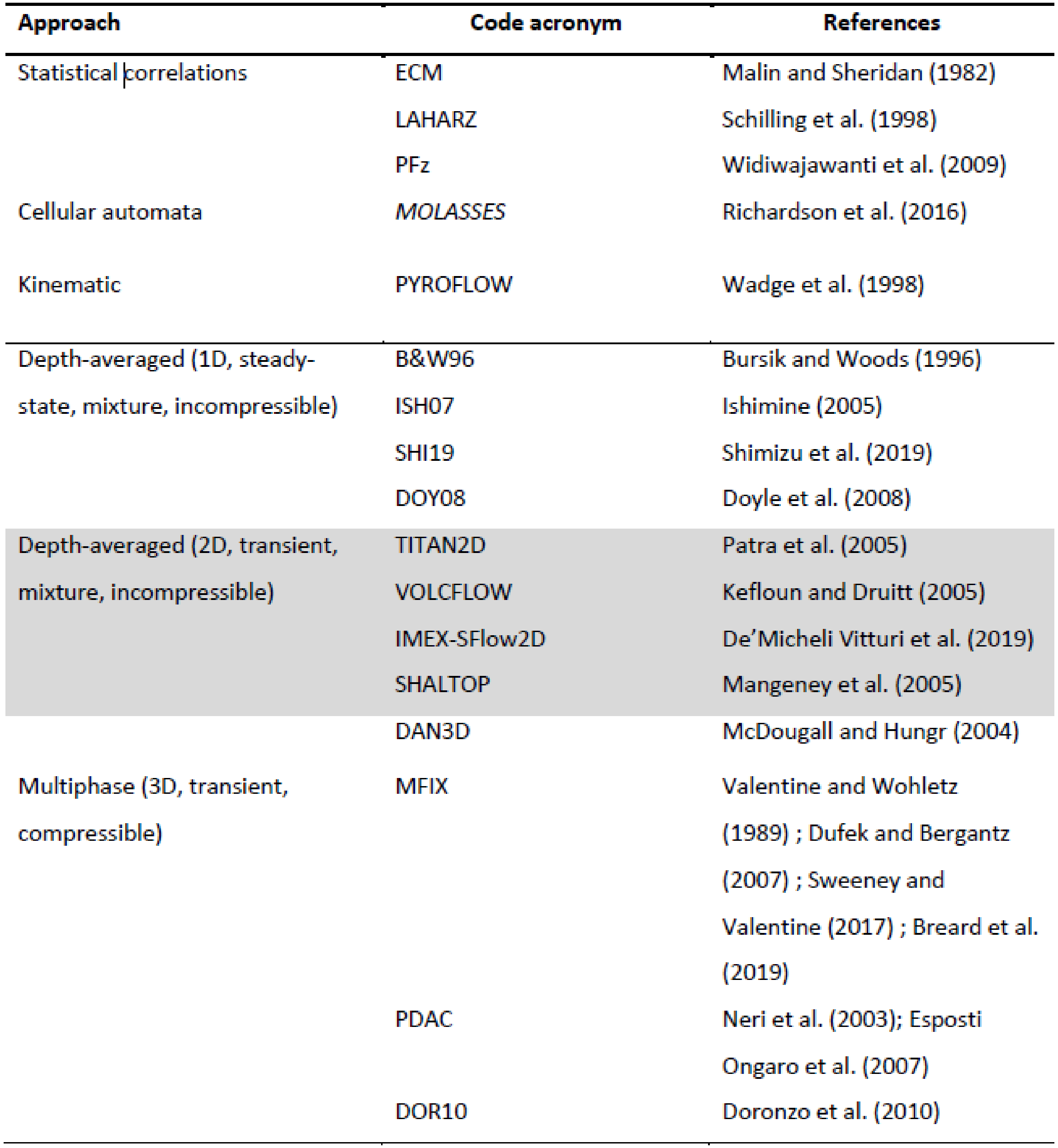

Approach	Code acronym	References
Statistical correlations	ECM	Malin and Sheridan (1982)
	LAHARZ	Schilling et al. (1998)
	PFz	Widiwajawanti et al. (2009)
Cellular automata	*MOLASSES*	Richardson et al. (2016)
Kinematic	PYROFLOW	Wadge et al. (1998)
Depth-averaged (1D, steady-state, mixture, incompressible)	B&W96	Bursik and Woods (1996)
	ISH07	Ishimine (2005)
	SHI19	Shimizu et al. (2019)
	DOY08	Doyle et al. (2008)
Depth-averaged (2D, transient, mixture, incompressible)	TITAN2D	Patra et al. (2005)
	VOLCFLOW	Kefloun and Druitt (2005)
	IMEX-SFlow2D	De'Micheli Vitturi et al. (2019)
	SHALTOP	Mangeney et al. (2005)
	DAN3D	McDougall and Hungr (2004)
Multiphase (3D, transient, compressible)	MFIX	Valentine and Wohletz (1989) ; Dufek and Bergantz (2007) ; Sweeney and Valentine (2017) ; Breard et al. (2019)
	PDAC	Neri et al. (2003); Esposti Ongaro et al. (2007)
	DOR10	Doronzo et al. (2010)

Statistical modeling of volcanic flows: PFz model

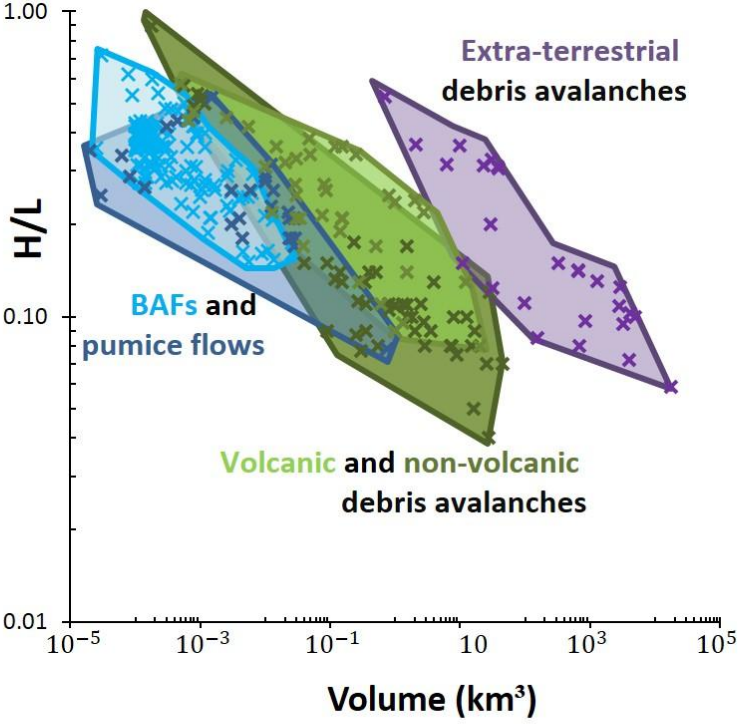

- Different types of flows have different H/L ratios, i.e., different mobility
- All types of flow show a decreasing H/L ratio with increasing volume, illustrating that large volume flows tend to be inherently more mobile…

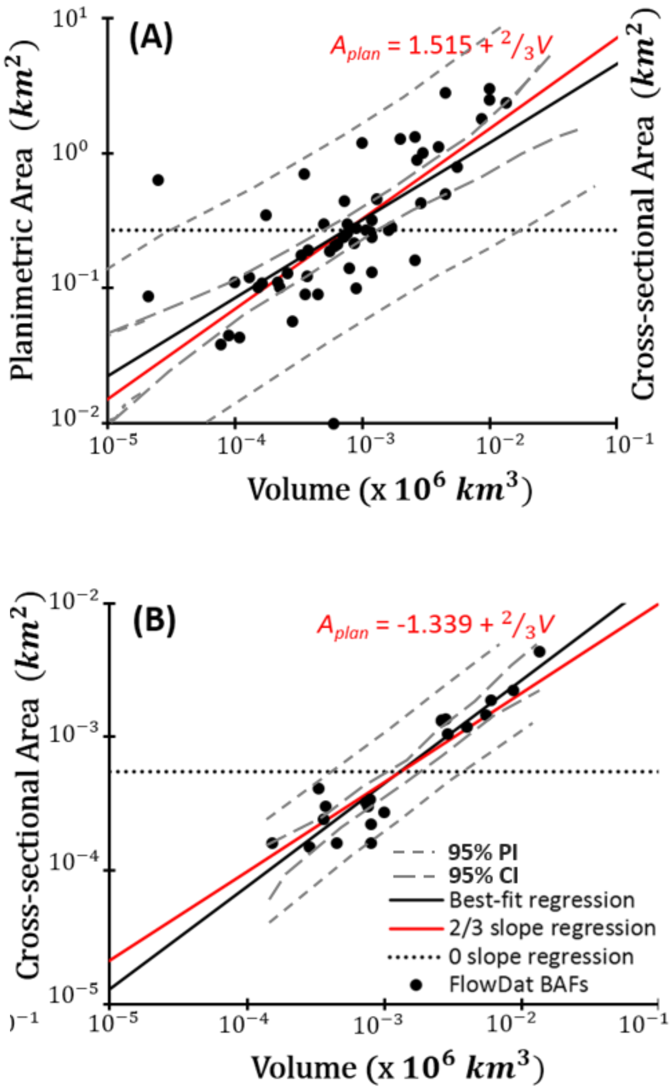

For PDCs only:

All PDCs:
A=0.05, B=33

PDCs > 2Mm³:
A=0.06, B=43

PDCs < 2Mm³:
A=0.04, B=32

FlowDat: Volcanic Mass Flow Database | U.S. Geological Survey

Geophysical Mass Flow Models

- **New class of geophysical mass flow (GMF) models** (Savage and Hutter, 1989)
→ **depth-averaged granular-flow model** on 3D terrain (Iverson and Denlinger, 2001)

▶ **TITAN2D model** developed at SUNY Buffalo, USA (Pitman et al., 2003; Patra et al., 2005)

▶ **VolcFlow model** written by K. Kelfoun (LMV, Clermont-Ferrand, France)

▶ **IMEX model** written by M. De' Michieli Vitturi et al. (INGV Pisa, Italy)

- **conservation equations** for mass (3) and momentum (4 and 5) → « **shallow-water »** models with **different resistance terms and numerical implementation**

$$\frac{\partial h}{\partial t} + \frac{\partial}{\partial x}(hu) + \frac{\partial}{\partial y}(hv) = 0 \qquad (3)$$

$$\frac{\partial}{\partial t}(hu) + \frac{\partial}{\partial x}(hu^2) + \frac{\partial}{\partial y}(huv) = gh\sin\alpha_x - \frac{1}{2}k_{actpass}\frac{\partial}{\partial x}(gh^2\cos\alpha) + \tau_x \qquad (4)$$

$$\frac{\partial}{\partial t}(hv) + \frac{\partial}{\partial x}(hvu) + \frac{\partial}{\partial y}(hv^2) = gh\sin\alpha_y - \frac{1}{2}k_{actpass}\frac{\partial}{\partial y}(gh^2\cos\alpha) + \tau_y \qquad (5)$$

Geophysical Mass Flow Models

- **New class of geophysical mass flow (GMF) models** (Savage and Hutter, 1989)

→ **depth-averaged granular-flow model** on 3D terrain (Iverson and Denlinger, 2001)

► **TITAN2D model** developed at SUNY Buffalo, USA (Pitman et al., 2003; Patra et al., 2005)

► **VolcFlow model** written by K. Kelfoun (LMV, Clermont-Ferrand, France)

► **IMEX model** written by M. De' Michieli Vitturi et al. (INGV Pisa, Italy)

- **conservation equations** for mass (3) and momentum (4 and 5) → « **shallow-water »** models with **different resistance terms and numerical implementation**

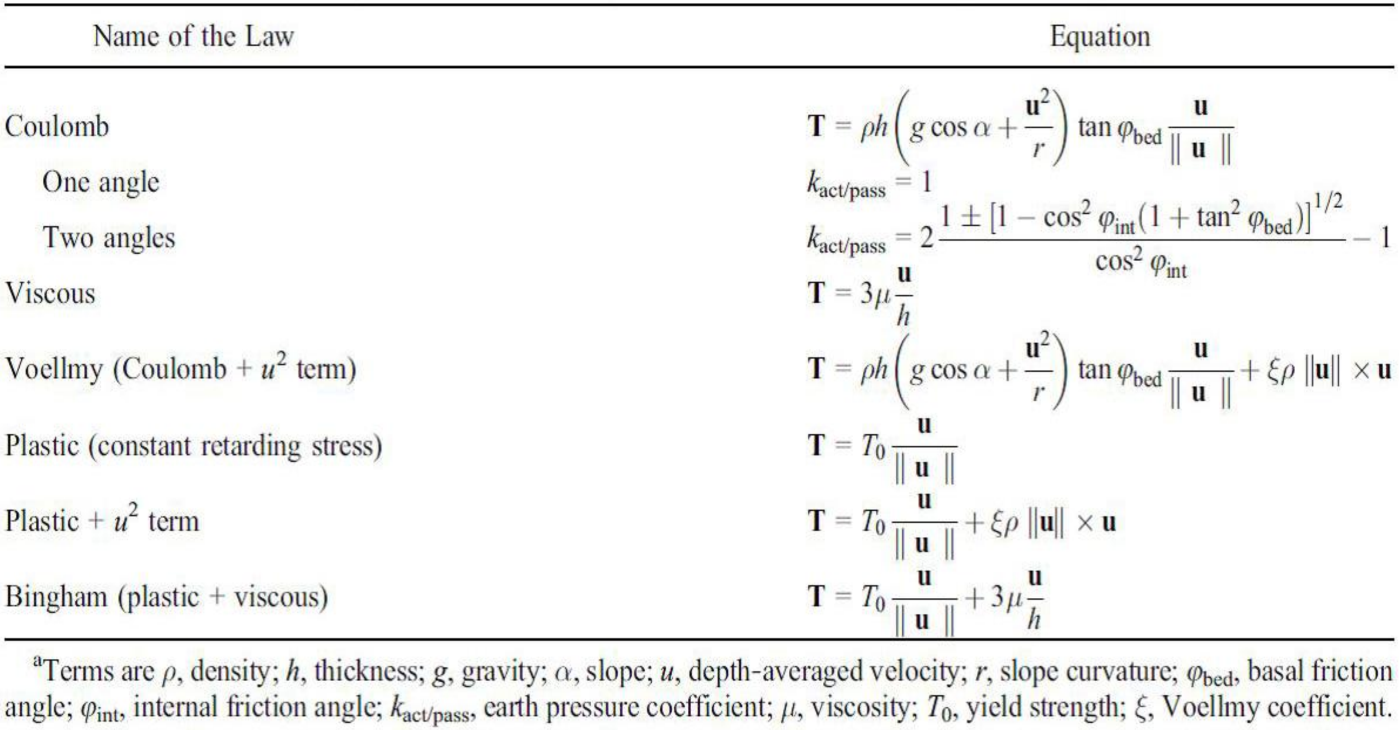

Name of the Law	Equation
Coulomb	$\mathbf{T} = \rho h\left(g\cos\alpha + \frac{\mathbf{u}^2}{r}\right)\tan\varphi_{\mathrm{bed}}\frac{\mathbf{u}}{\lVert \mathbf{u} \rVert}$
One angle	$k_{\mathrm{act/pass}} = 1$
Two angles	$k_{\mathrm{act/pass}} = 2\frac{1 \pm [1 - \cos^2\varphi_{\mathrm{int}}(1 + \tan^2\varphi_{\mathrm{bed}})]^{1/2}}{\cos^2\varphi_{\mathrm{int}}} - 1$
Viscous	$\mathbf{T} = 3\mu\frac{\mathbf{u}}{h}$
Voellmy (Coulomb + u^2 term)	$\mathbf{T} = \rho h\left(g\cos\alpha + \frac{\mathbf{u}^2}{r}\right)\tan\varphi_{\mathrm{bed}}\frac{\mathbf{u}}{\lVert \mathbf{u} \rVert} + \xi\rho\lVert\mathbf{u}\rVert \times \mathbf{u}$
Plastic (constant retarding stress)	$\mathbf{T} = T_0\frac{\mathbf{u}}{\lVert \mathbf{u} \rVert}$
Plastic + u^2 term	$\mathbf{T} = T_0\frac{\mathbf{u}}{\lVert \mathbf{u} \rVert} + \xi\rho\lVert\mathbf{u}\rVert \times \mathbf{u}$
Bingham (plastic + viscous)	$\mathbf{T} = T_0\frac{\mathbf{u}}{\lVert \mathbf{u} \rVert} + 3\mu\frac{\mathbf{u}}{h}$

[a] Terms are ρ, density; h, thickness; g, gravity; α, slope; u, depth-averaged velocity; r, slope curvature; φ_{bed}, basal friction angle; φ_{int}, internal friction angle; $k_{\mathrm{act/pass}}$, earth pressure coefficient; μ, viscosity; T_0, yield strength; ξ, Voellmy coefficient.

Geophysical mass flow models

	TITAN 2D	VolcFlow	IMEX
Developers	SUNY Buffalo USA	K. Kelfoun, LMV, Clermont-Fd, France	De' Michieli Vitturi et al. (INGV Pisa, Italy)
Platform	Linux/online	Windows/Linux	Linux/online
Numerical framework	Adaptive finite volume scheme	Finite volume solver	Finite volume solver (Runge-Kutta)
Rheological law	Mohr-Coulomb, Voellmy, Pouliquen, Two-Phase (water + solid)	Any user-defined laws, Two-phase (dense + dilute)	Multiple (11 different laws) (+ air entrainment)
Processing	Parallel	Single	Parallel
Source code	Accessible	No access	Accessible
Digital elevation data	GRASS GIS/GDAL	Golden Software Surfer™	GDAL

Mohr-Coulomb frictional rheology

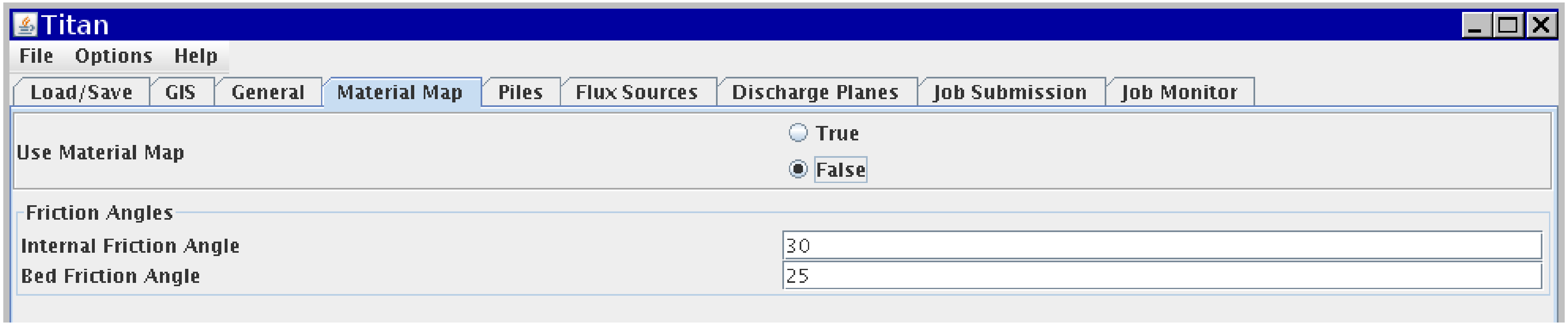

Use Material Map ○ True ● False

Friction Angles

Internal Friction Angle 30

Bed Friction Angle 25

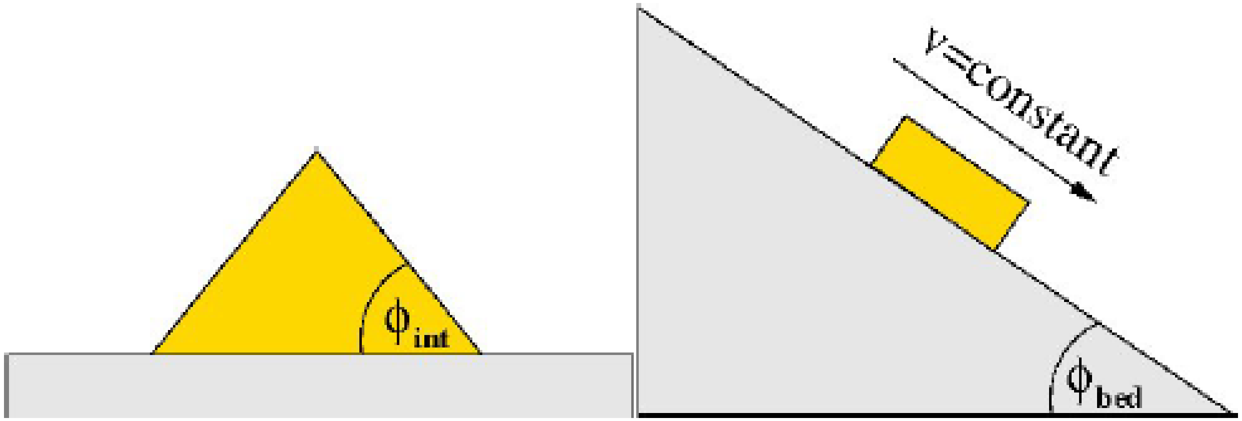

- The internal friction angle ϕ_{int}, is the steepest angle that the upper surface of a conical pile of dry sand can make with respect to the horizontal plane it is resting on.
- The bed (also known as basal) friction angle, ϕ_{bed}, is the angle that a plane needs to be inclined so that a block of material will slide downslope at a constant speed.

But…PDC flow rheology varies along flow (deposit and morphology characteristics vary laterally)

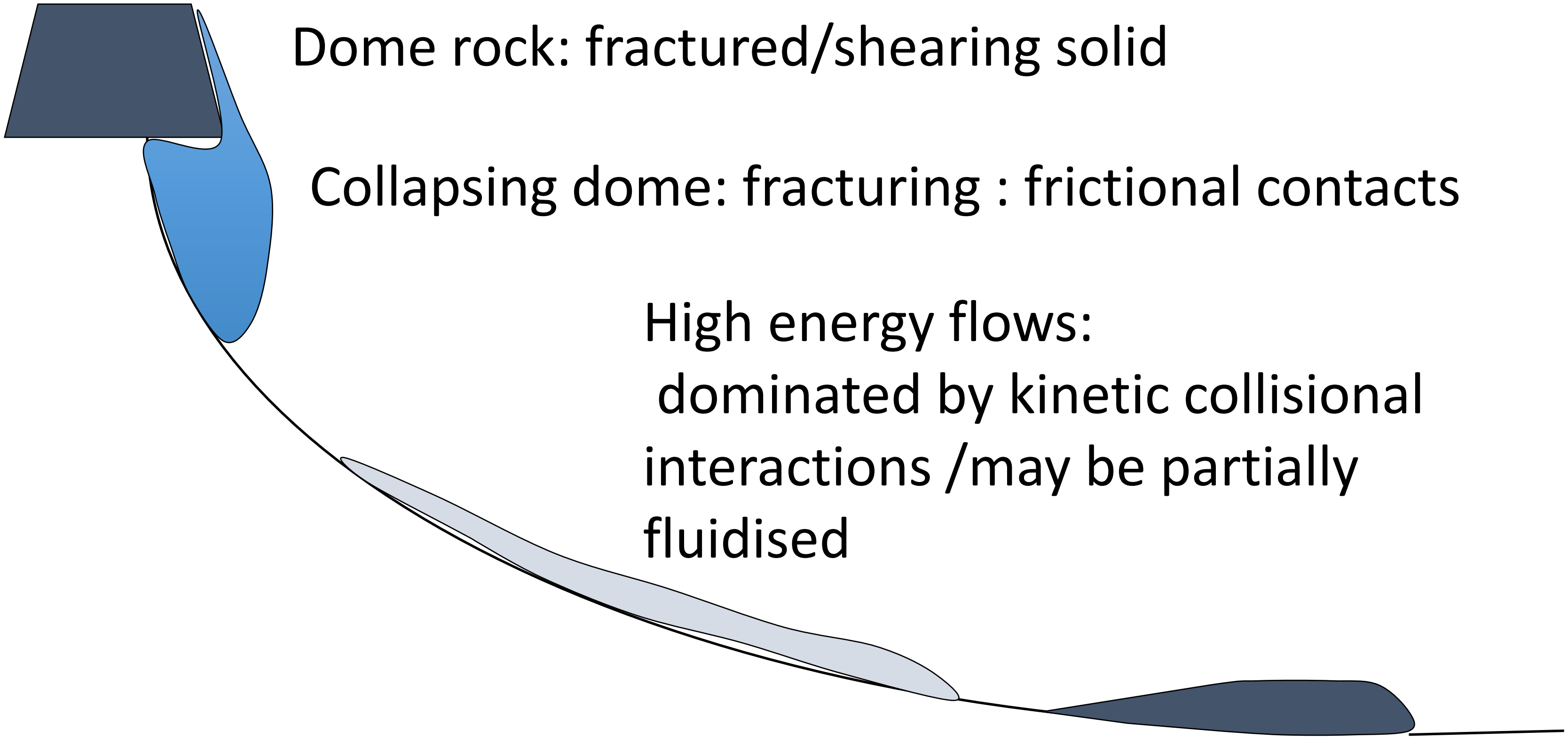

Dome rock: fractured/shearing solid

Collapsing dome: fracturing : frictional contacts

High energy flows:
dominated by kinetic collisional interactions /may be partially fluidised

Stopping flow:
frictional contacts dominate

But…PDC flow rheology varies along flow (deposit and morphology characteristics vary laterally)

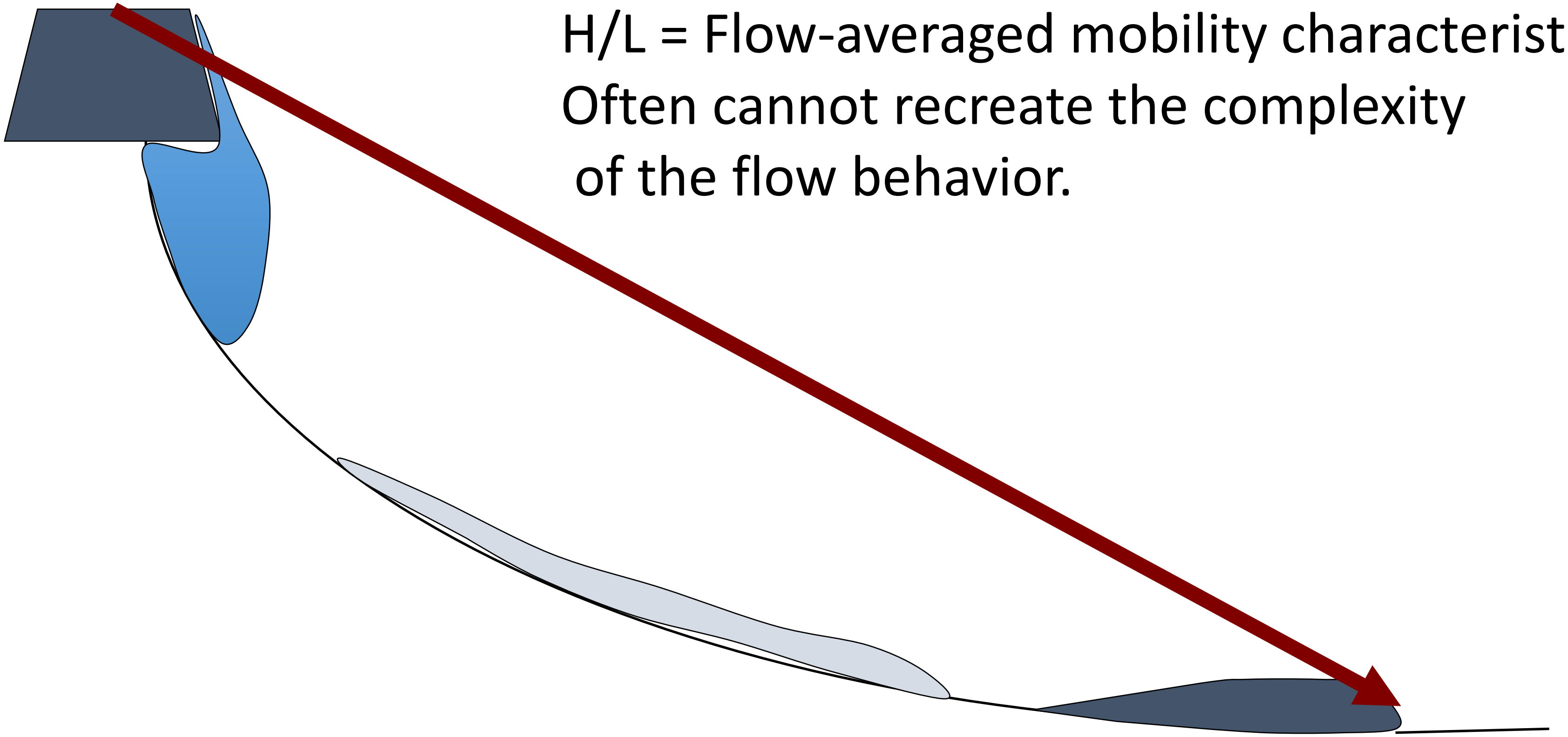

H/L = Flow-averaged mobility characteristic
Often cannot recreate the complexity
of the flow behavior.

The next generation of models will have variable rheology……

Sensitivity tests: Mohr-Coulomb rheology

Single friction angle: 16.7°

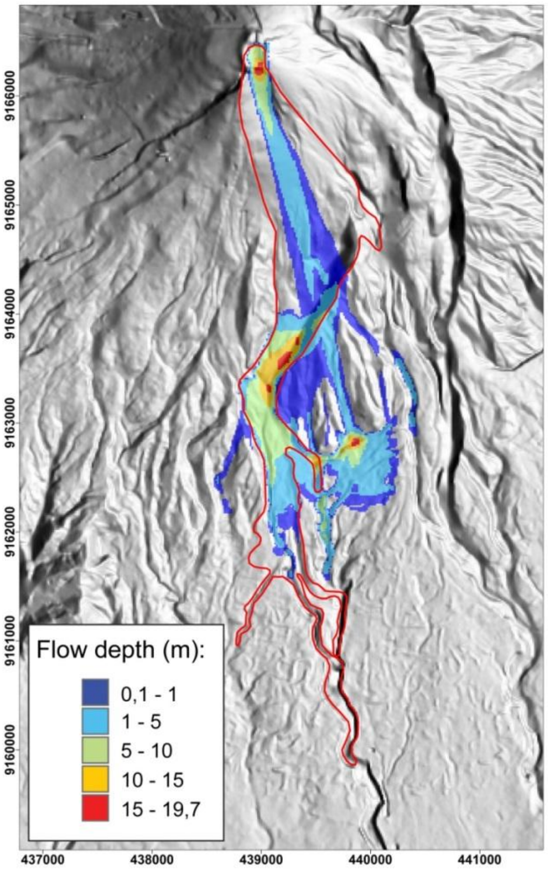

Jaccard Fit: **18.2%**

Single friction angle: 20°

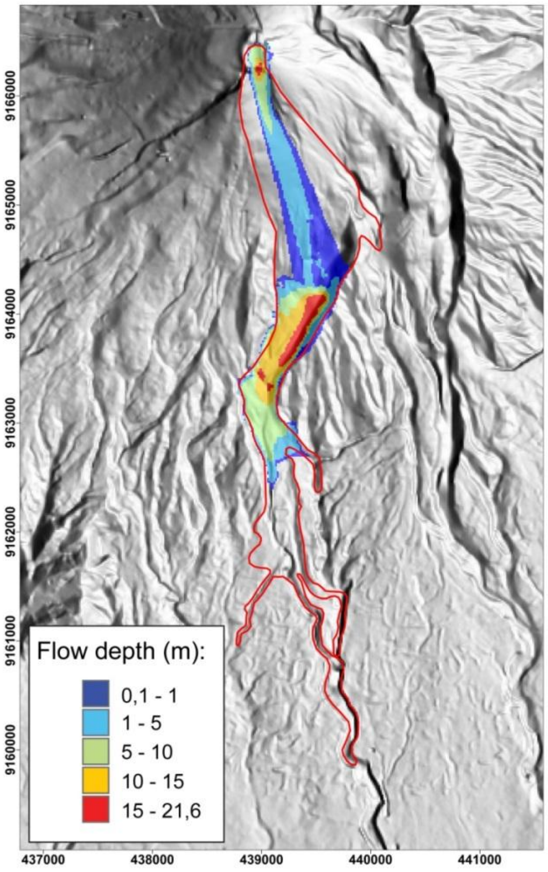

Jaccard Fit: **32%**

Varying friction angle: 24-10°

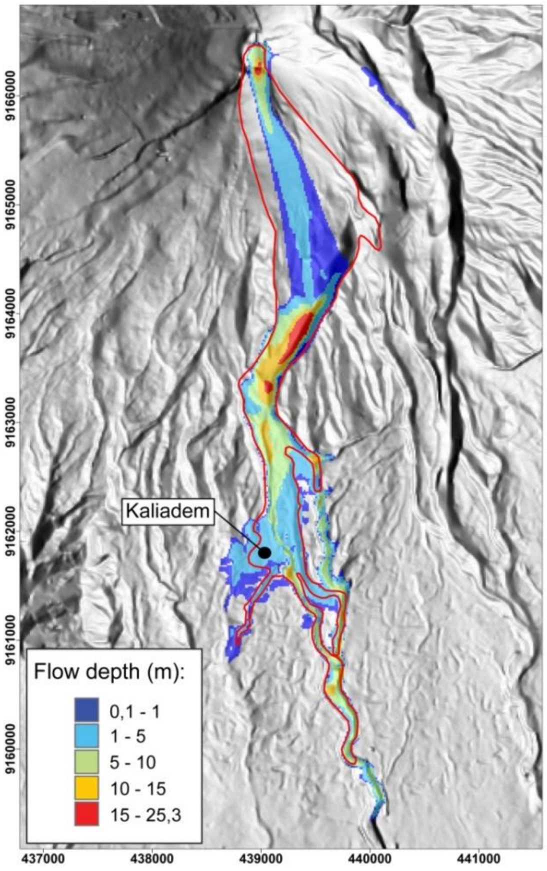

Jaccard Fit: **72.3%**

Using a single bed friction angle, simulated flows either spilled over ~200-m-high ridges or covered only half of the area calculated for the actual event…

Sensitivity tests: DEM resolution

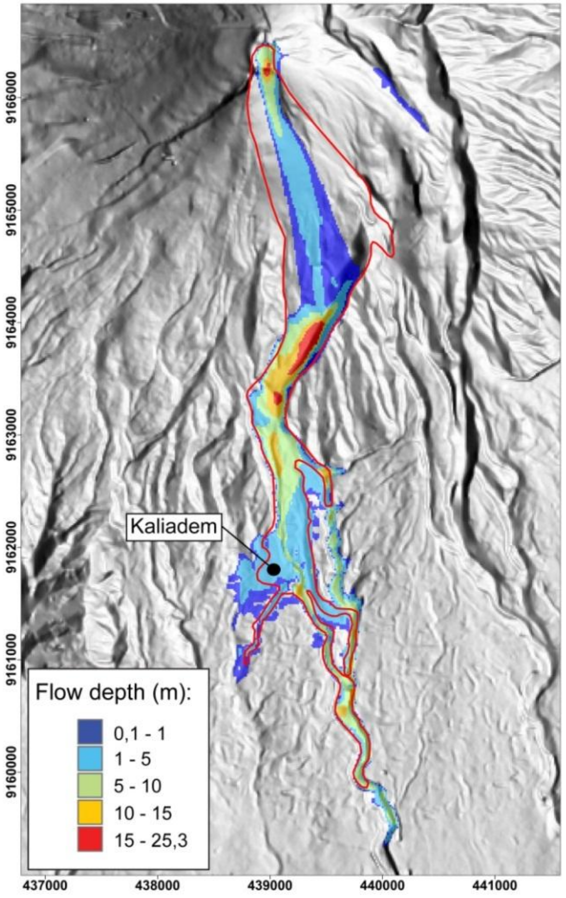

Local DEM

15 m spatial resolution
± 9 m vertical accuracy

Jaccard Fit: **72.3%**

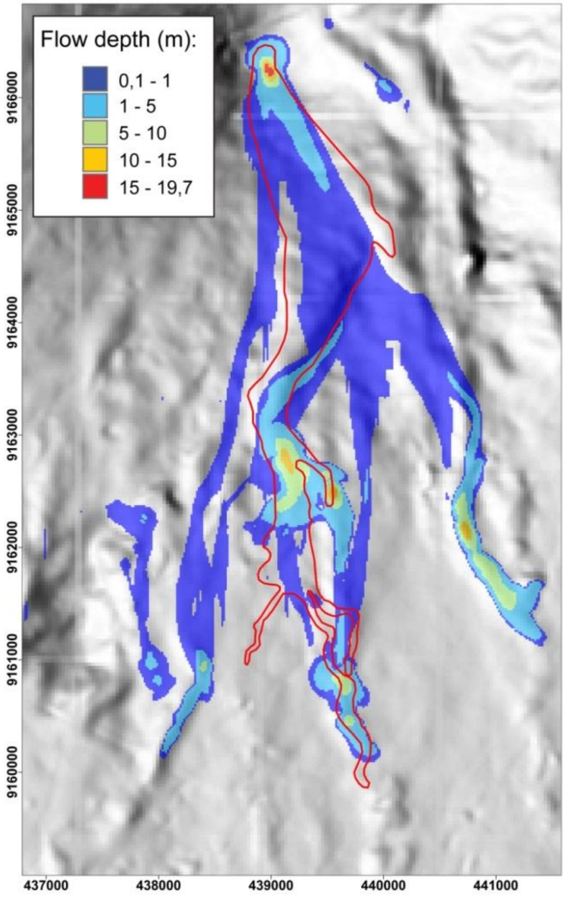

ASTER GDEM

~30 m spatial resolution
± 11 m vertical accuracy

Jaccard Fit: **25.6%**

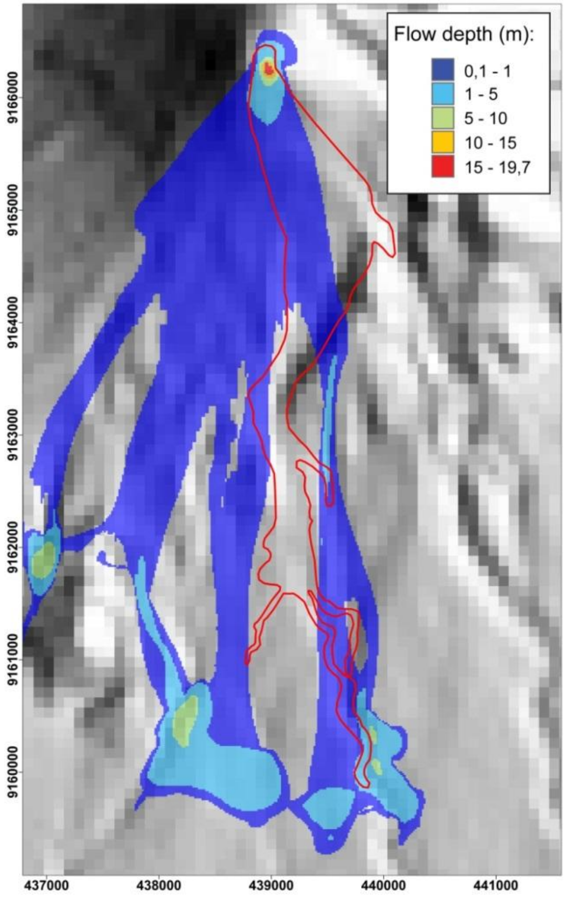

SRTM WRS-2

90 m spatial resolution
± 10 m vertical accuracy

Jaccard Fit: **7%**

Multiphase flow models

- PDAC (Pyroclastic Dispersal Analysis Code) *Esposti Ongaro et al. (INGV Pisa, Italy)*

Eulerian multiphase transport equations of mass, momentum, and enthalpy of a gas-pyroclast mixture formed by a continuous multicomponent gas phase and *n*-solid particle phases representative of pyroclasts, with each phase characterized by size, density, specific heat, and thermal conductivity…

- Mass balance:

$$\frac{\partial}{\partial t}\varepsilon_g\rho_g + \nabla\cdot(\varepsilon_g\rho_g\mathbf{v}_g) = 0; \qquad \frac{\partial}{\partial t}\varepsilon_g\rho_g y_m + \nabla\cdot(\varepsilon_g\rho_g y_m\mathbf{v}_g) = 0$$

$$\frac{\partial}{\partial t}\varepsilon_k\rho_k + \nabla\cdot(\varepsilon_k\rho_k\mathbf{v}_k) = 0$$

- Momentum balance:

$$\frac{\partial}{\partial t}\varepsilon_g\rho_g\mathbf{v}_g + \nabla\cdot(\varepsilon_g\rho_g\mathbf{v}_g\mathbf{v}_g) = -\varepsilon_g\nabla P_g + \nabla\mathbf{T}_g + \varepsilon_g\rho_g\mathbf{g} + \sum_{s=1}^{N} D_{g,s}(\mathbf{v}_s - \mathbf{v}_g)$$

$$\frac{\partial}{\partial t}\varepsilon_k\rho_k\mathbf{v}_k + \nabla\cdot(\varepsilon_k\rho_k\mathbf{v}_k\mathbf{v}_k) = -\varepsilon_k\nabla P_g + \nabla\mathbf{T}_k + \varepsilon_k\rho_k\mathbf{g} - D_{g,k}(\mathbf{v}_k - \mathbf{v}_g) + \sum_{s=1}^{N} D_{k,s}(\mathbf{v}_s - \mathbf{v}_k)$$

- Enthalpy balance:

$$\frac{\partial}{\partial t}\varepsilon_g\rho_g h_g + \nabla\cdot(\varepsilon_g\rho_g h_g\mathbf{v}_g) = \varepsilon_g\left(\frac{\partial P_g}{\partial t} + \mathbf{v}_g\cdot\nabla P_g\right) + \nabla\cdot(\kappa_{ge}\varepsilon_g\nabla T_g) + \sum_{s=1}^{N} Q_s(T_s - T_g)$$

$$\frac{\partial}{\partial t}\varepsilon_k\rho_k h_k + \nabla\cdot(\varepsilon_k\rho_k h_k\mathbf{v}_k) = \nabla\cdot(\kappa_{ke}\varepsilon_k\nabla T_k) - Q_k(T_k - T_g)$$

With ε is the phase volumetric fraction, y is the mass fraction of a gas species, $\mathbf{v}$ is the velocity vector, ρ is microscopic density, P is the thermodynamic pressure, R is the gas constant divided by the effective gas molecular weight, h is the phase enthalpy, T is the temperature, $\mathbf{T}$ is the stress tensor, κ is the thermal diffusivity coefficient, Cp is the specific heat at constant pressure, G(εg) is the solid compressive modulus. Subscript g indicates the gas phase, k (running from 1 to N) the solid phases, m (running from 1 to M) the gas species. μ_g is the dynamic gas viscosity coefficient, μ_{ge} indicates effective gas viscosity accounting for turbulent subgrid transport, μ_k is a solid viscosity coefficient (depending only on particle size).

Interphase exchange coefficients: $D_{g,k}$, $D_{k,j}$, Q_g, Q_s

Multiphase flow models

- PDAC (Pyroclastic Dispersal Analysis Code) *Esposito Ongaro and Neri (INGV Pisa, Italy)*

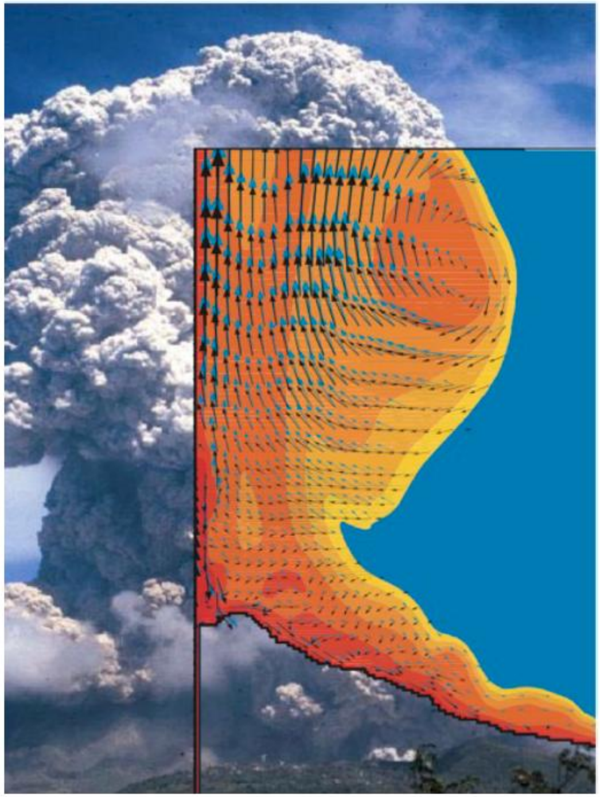

Clarke et al. (2002). Nature

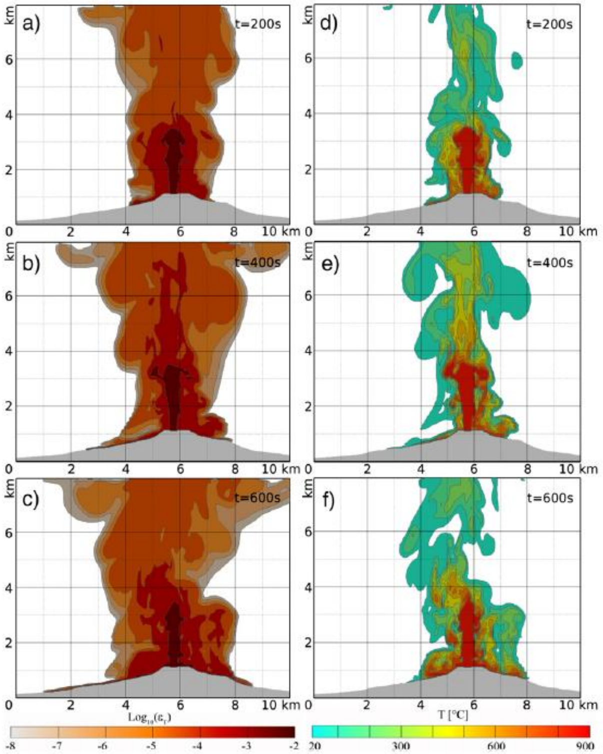

Esposti Ongaro et al. (2008). JVGR

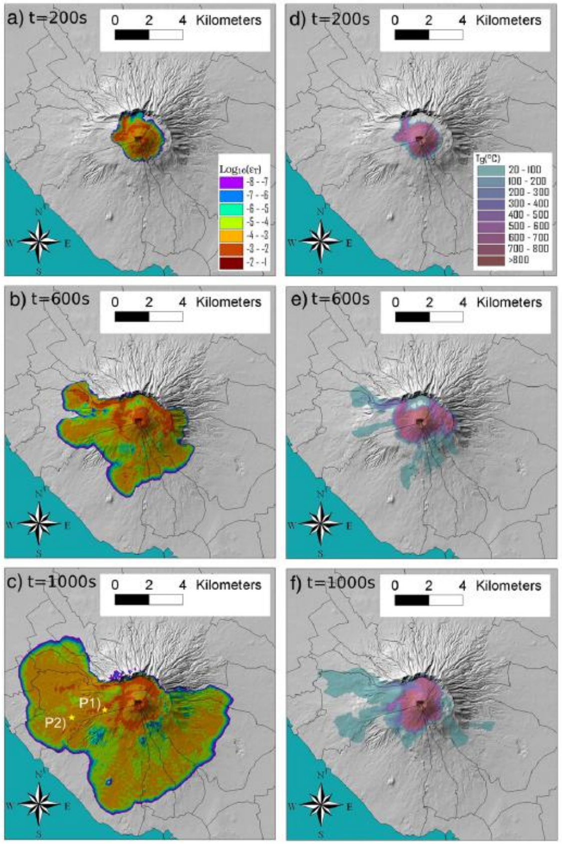

PDAC 2D with one gas phase coupled to a solid phase with different grain sizes

PDAC 3D with (a,b, c) total volume particle fractions and (d, e and f) gas temperatures

Multiphase flow models: MFIX

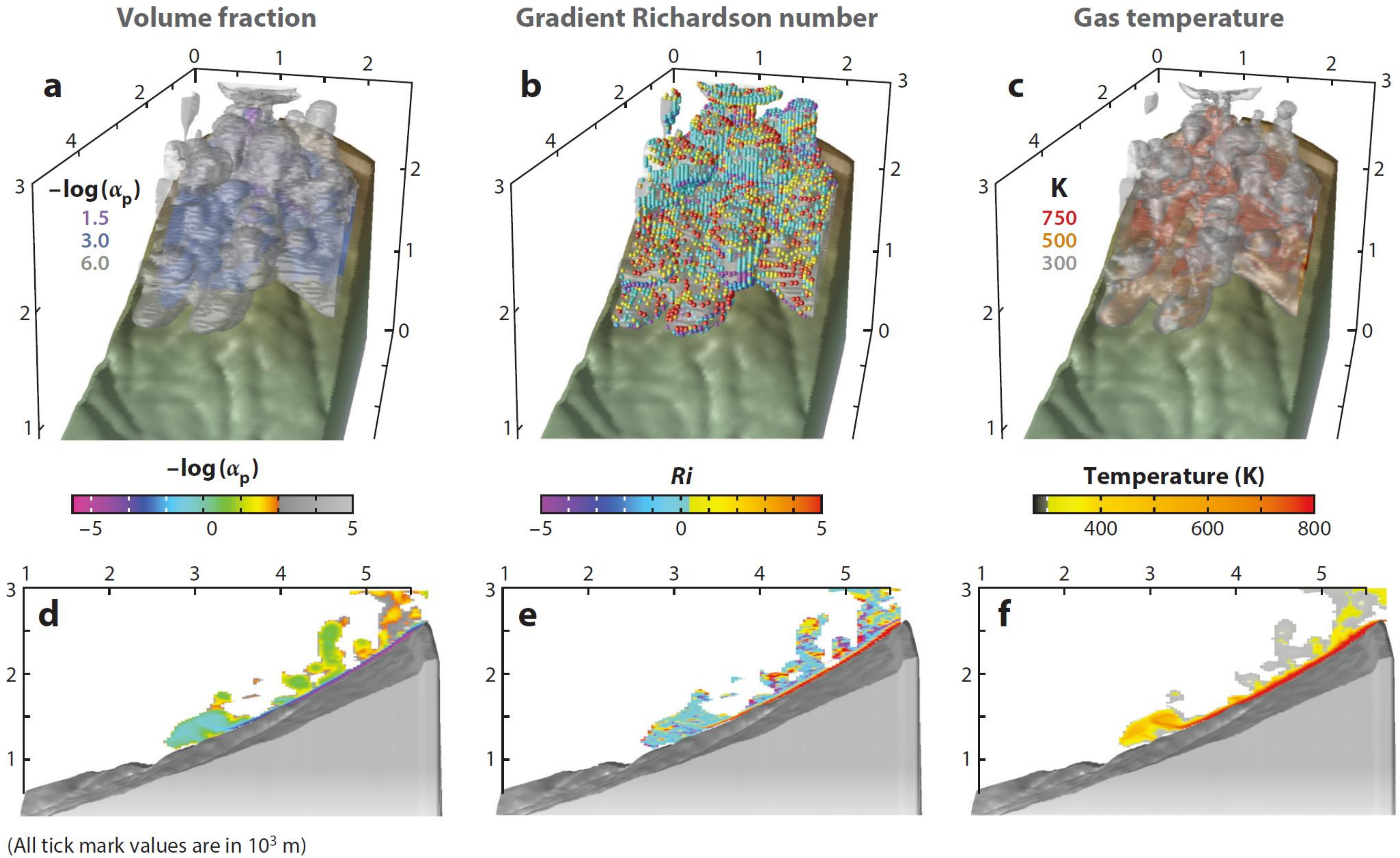

Multiphase simulation of a pyroclastic density current in the Juive Grande drainage of Tungurahua, Ecuador (70 s after initiation). This simulation has an initial particle volume fraction of 0.3 and comprises 0.1-mm and 1-mm particles. The simulation shows the heterogeneity of pyroclastic density currents and the entrainment efficiency. The concentrated bed load remains hot as the large density stratification in this region of the flow inhibits mixing owing to shear. (*after Benage et al., JGR, 2016)*